Biochemistry and Biophysics Reports 40 (2024) 101866

Contents lists available at ScienceDirect

Biochemistry and Biophysics Reports

journal homepage: www.elsevier.com/locate/bbrep

Molecular dynamics studies reveal the structural impacts of LRRK2 R1441C and LRRK2 D1994A mutations in Parkinson's disease

Ramisha A. Rahman [a], Bushra Zaman [a,b], Md Shariful Islam [a,c], Md Harunur Rashid [a,*]

[a] Department of Mathematics & Physics, North South University, Dhaka, Bangladesh
[b] Department of Neurobiology and Developmental Sciences, University of Arkansas for Medical Sciences, Arkansas, United States
[c] Department of Chemistry and Biochemistry, New Mexico State University, New Mexico, United States

ARTICLE INFO

Keywords:
Parkinson's disease
LRRK2
Molecular dynamics
R1441C mutation
D1994

ABSTRACT

Parkinson's Disease (PD) is a continuingly deteriorating neurological ailment affecting over 8.5 million patients globally as of 2019, and the numbers are expected to keep rising. To aid in identifying therapeutic targets, molecular dynamics simulations are convenient and cost-effective methods for enriching our knowledge of the molecular pathophysiology of diseases. Many proteins and their corresponding mutations have been identified to contribute to this disease, of which Leucine-rich repeat kinase 2 (LRRK2) is accountable for a significant percentage. Several mutations involving the domains in LRRK2 have been studied, which are known to interfere with various enzymatic processes, ultimately leading to trademark features of PD like aggregation of protein inclusions called Lewy Bodies (LBs), mitochondrial dysfunctions, etc. The precise molecular mechanism of the mutations' pathophysiology is still unclear. This research article looks at the structural effects of mutations, namely the R1441C and D1994A mutations, on the surrounding residues in the protein, offering novel insights into pathophysiological changes at an atomistic level. Our results indicate a gain of electrostatic interactions with a stable αβ motif within the LRR-Roc linker, amongst other changes. This article also highlights the potential involvement and importance of the αβ motif in LRRK2 associated PD.

1. Introduction

Parkinson's Disease (PD) is a neurological disorder distinguished by the continuous decline of motor and nonmotor functions [1]. With a prevalence only second to Alzheimer's Disease amongst neurodegenerative diseases, PD is a chronic ailment that is progressively debilitating for patients since onset. Prominent motor effects include bradykinesia, postural instability, and loss of motor control [1]. Clinical manifestations also include non-motor features such as depression, loss of memory, sleep disorders, etc., which may even precede the quintessential motor features of PD [2]. These symptoms arise due to degeneration of dopaminergic neurons residing in a location of the brain involved with movement control, called the substantia nigra pars compacta [3].

At the molecular level, a prominent characteristic of PD is the presence of fibrillar inclusions, also known as Lewy bodies. These inclusions have been extensively examined to determine their role in the brains of PD patients [4]. Discovered over a century ago, a vast array of information is now available to us about the constituents of Lewy bodies, of which the presynaptic protein ɑ-synuclein is of particular importance. The aggregation of this protein causes neurotoxicity through a number of ways, a significant mechanism being its disruption of neurotransmitter release [5,6].

While a significant proportion of PD cases occur with no specific etiology, a small percentage (10–15 %) [7] is hereditary and has been linked to mutations in around 20 known genes [8,9]. These hereditary forms of PD, also known as monogenic PD, is the result of autosomal dominant and autosomal recessive mutations in various causative genes. Mutations implicated in autosomal dominant PD involve *SNCA, LRRK2,* and *VPS35* genes [10,11], while autosomal recessive PD involves mutations in *Parkin, PINK1, DJ-1,* and *DNAJC6* genes [12].

The principal cause of autosomal dominant PD at later ages is ascribed to mutations in the *LRRK2* gene, with clinical attributes akin to those associated with late-onset sporadic PD [13–16]. Previous studies have identified LRRK2 cellular localization in Parkinson's patients and LRRK2 as a known constituent of Lewy bodies [17]. As a sizable multifunctional protein weighing around 280 kD, *LRRK2* contains two significant catalytic domains – the GTPase and kinase domains [15]. The prevalence of certain multiprotein domains, including a characteristic

* Corresponding author.
E-mail address: harunur.rashid01@northsouth.edu (M.H. Rashid).

https://doi.org/10.1016/j.bbrep.2024.101866
Received 15 September 2024; Received in revised form 30 October 2024; Accepted 6 November 2024

leucine-rich domain, and a WD40 repeat, have also been noted [18–22] (Fig. 1).

Mutations within enzymatic domains have been associated with affecting the mechanistic pathways of the disease [20,21]. Linked with approximately 1 % of idiopathic cases of late-onset PD alongside 5–6% of hereditary PD globally, the prominence of the G2019S mutation in the kinase domain has been deemed the greatest [23]. G2019S *LRRK2* cases comprise LB formation and incomplete penetrance, which is still present at later ages [24]. On the other hand, a variable LB formation and nearly complete penetrance is exhibited by GTPase domain mutations such as R1441C/G [13,14]. This has led to speculations regarding the unique pathways employed by these mutations. Furthermore, multiple pieces of evidence indicate the interdependent regulation of LRRK2 GTPase and kinase enzyme activities, which contributes to a deeper comprehension of the cellular mechanistic pathways associated with LRRK2 functions [25,26]. The physiological function of LRRK2 is linked with lysosomal autophagy, cytoskeletal balance, translation of proteins, mitochondrial homeostasis, etc. [22,25,27–30].

Investigation of the R1441C mutation's effects has been vast and extensive. Wszolek and colleagues presented their findings on the degeneration of pigmented neurons in the Substantia Nigra and Locus Coeruleus regions of the brain, along with an observed increase in fibrous growth of glial cells [13,31]. Other studies have found that the clinical manifestations of the mutation were akin to those exhibited in idiopathic PD [32]. Due to the multiple mutations observed in the residue 1441, it has been studied through various models, including mice and fruit flies to navigate its significance [33]. Tong et al. used genetically modified knock-in mice to demonstrate that the R1441C mutation significantly disrupted the dopamine receptor D2 in the brain and modified stimulatory effects on dopaminergic neurotransmission [34]. The presence of the mutation in the Roc domain induces lowered GTPase activity, although the residue in question lies outside the GTP binding pocket, suggesting indirect effects of the mutated residue [35]. Nevertheless, the residue lies on the dimerization interface, which is essential for optimal GTPase activity, suggesting a pathophysiological mechanism to exist in this regard [36,37]. Potentially targeting this mutation's

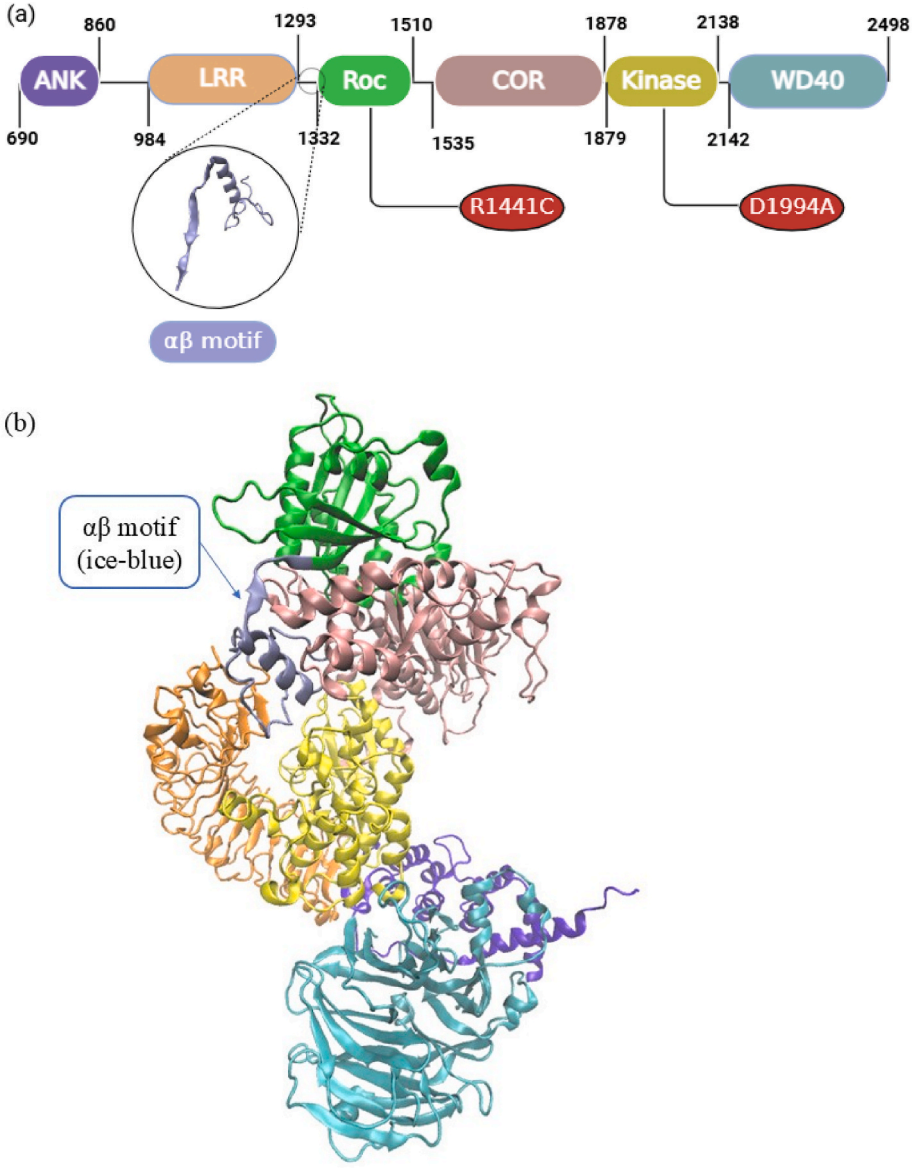

Fig. 1. (a) Domains of the LRRK2 protein, including numbers of the residues they comprise. The positions of two residues have been highlighted in red oval as these mutations were studied in this paper. (b) LRRK2 protein (PDB ID: 7LHW) represented in the New-Cartoon model with different domains shown in different colors, namely; the Kinase domain in yellow, Roc (Ras of complex) domain in green, COR (C-terminal of Roc) domain in pink, WD40 domain in cyan, LRR (Leucine-rich-repeat) domain in orange and ANK (Ankyrin repeat) domain in magenta. The residues between the LRR and Roc domains have been shown in ice blue color.

effects in PD comes with the added advantage of specificity and reduced off-target effects, since it is one of the only four Roc GTPases found in humans [38]. A detailed structural analysis of the mutated protein may aid in further knowledge regarding its effects manifested clinically in patients, potentially unlocking new avenues of targeted treatment.

Irrespective of the mutation's location, all LRRK2 mutations associated with PD have been known to exert an effect on kinase activity [15]. This observation suggests a link between mutations in the GTPase enzymatic domain and kinase domain, which led to the discovery of the two being spatially close to each other through in-situ studies [39]. It is also widely held that diminished GTPase activity results in heightened kinase activity, although this remains inconclusive [35]. An artificial mutation D1994A located in the kinase domain has been implemented in the past for its inhibition of kinase activity. While several double mutation studies of a gain of function mutation such as G2019S and kinase dead mutation D1994A have been conducted previously, no research has been performed to identify any changes induced by a kinase dead mutant on a GTPase affecting mutation.

The steep increase in number of PD patients globally is alarming, with an estimated doubling to 13 million patients by 2040 [40]. Despite the threat of a PD pandemic, our resources for combat are inadequate, with symptomatic treatment still the mainstay of treatment. While further research is warranted to develop better therapeutics to halt disease progression, genetic models of LRRK2 pose several limitations [41]. One of the more promising approaches to investigating the structural effects of genetic mutations is molecular dynamics simulations, as seen in our previous studies [42–46]. These enable us to investigate how regions within mutated proteins may interact with adjacent regions in the protein system [47].

In this study, LRRK2 and R1441C mutant LRRK2 systems are analyzed to reveal structural modifications which may be posited to explain the consequent lowering of GTPase activity. Additionally, the structural effects of D1994A on neighboring residues are also evaluated to provide insight into the therapeutic potential of kinase inhibitors for mutations in the GTPase domain. This is further examined through introduction of both the mutations and analysis of the resulting system. Our results are complementary to experimental findings, offering novel insight conducive to the development of novel therapeutics.

2. Material and methods

Simulations were performed for the LRRK2 protein (PDB ID: 7LHW) and its mutations associated with Parkinson's disease. The PDB structure of 7LHW incorporates three natural variants and was left unchanged and considered as the wild type of LRRK2 (LRRK2-WT) [48]. Point mutations were further introduced into the intact PDB ID: 7LHW (LRRK2-WT) structure for studying the mutant systems following simulation. The simulations employed NAMD (Nanoscale Molecular Dynamics) 2.12 [49] and the CHARMM36 force field [50]. Atmospheric conditions of temperature 298K and semi-isotropic pressure of 1 atm were conserved throughout the simulations. PME (particle-mesh Ewald) was utilized for calculation of long-range electrostatic interactions, for which a cutoff limit of 12 Å was employed. The simulation was performed using periodic boundary conditions, and an integration time step of 2 fs. Lennard-Jones potential was used in calculation of van der Waals interactions, also with a cutoff value at 12 Å, and a smooth switching function in place as 10 Å was crossed.

Each protein system was confined in a periodic orthorhombic box with dimensions ~180 × 180 × 180 Å in size. KCl was added for neutralization and to achieve the physiological buffer concentration of 150 mM/L. The resulting simulation system comprised of 383 K^+ and 384 Cl^- ions, along with 35,064 water molecules for the LRRK2 protein. The remaining three systems also contained similar numbers of water molecules and ions.

The input files for each of the simulations were created using CHARMM GUI [50,51]. Mutations were introduced by manipulating the PDB. For the LRRK2-WT model, no mutation was introduced. In the case of the R1441C mutant, a mutation of Arginine to Cysteine was introduced at the 1441 residue of PDB ID: 7LHW. Similarly, for the D1994A model, an Aspartic acid to Alanine mutation was introduced at the residue 1994 of PDB ID: 7LHW. For the final simulation consisting both mutations, two mutations as mentioned above were introduced in the LRRK2 model (PDB ID: 7LHW).

All systems underwent equilibration over 10 ns, along which conformational restraints were decreased in stages. Upon the end of equilibration, the simulations of LRRK2 system as well as the LRRK2 [R1441C] and LRRK2[D1994A] were run for 500 ns to facilitate a study of structural changes in LRRK2 mutant proteins compared to the Wild type. The system with a double mutation (LRRK2[R1441C/D1994A]) was run for 100 ns. These structural changes were observed through visualization and distance analyses of the simulated systems were performed using VMD (Visual Molecular Dynamics) 1.9.3 [52]. Figures were created using XMGrace plotting tool.

3. Results

The region between the LRR and Roc domain (Fig. 1), also known as the LRR-Roc linker, consists of a strong conformation of a connected α helix and β pleated sheet. The β sheet extends into the beginning of the Roc domain, so this motif which is further investigated in this article is referred to as the αβ motif hereafter.

3.1. Electrostatic interactions compared in LRRK2-WT and LRRK2 [R1441C] proteins

The R1441 residue lies in the Roc domain (Fig. 1). In the LRRK2-WT simulated model, we observe that the sidechain nitrogen atom of R1441 interacts with the carbonyl oxygen of M1409 in the same domain, whereas the other sidechain nitrogen atom of R1441 makes an N_2–O interaction with the carbonyl oxygen of W1791, located in the COR Domain (Fig. 2(a)).

To assess the stability of the interaction, we plotted the interacting distances over the course of the entire simulation and found a strong interaction of 2.8 ± 0.3 Å between R1441 and residues M1409 and W1791 (red and green distances in Fig. 3, respectively) in LRRK2-WT.

Notably, both of these interactions were completely absent in the LRRK2[R1441C] mutant (Fig. 2(b)). In contrast, the R1412 residue in the Roc domain forms a strong charged interaction with the D1307 residue (Fig. 4) in the RC mutant system, which is located within a strong motif comprised of a beta-sheet and an alpha-helix between the LRR and the Roc domain (Ice blue color in Fig. 1).

Since arginine contains two nitrogen groups in its side chain which flip during the course of the simulation, the C_Z-C_g atomic distance was plotted instead, which represents a strong charge interaction as shown in Fig. 4.

Upon introduction of the R1441C residue mutation, two interactions, R1441-M1409 and R1441-W1719 within the Roc domain and with the COR domain, respectively, were lost. The interaction R1412-D1307 with the αβ motif (Ice Blue region) was formed instead. We speculated how that would translate to the stability of the domains involved, and thus plotted the RMSD (root mean square deviation) of the Roc and the COR domains Fig. 5.

The RMSD plot shows the COR domain to shift more than 2.5 Å, whereas the Roc domain was found to be quite stable towards the αβ motif, perhaps due to the stable interaction of R1412-D1304. The separation of these two domains is also consistent with the findings of previous studies of low GTPase activity, as induced by R1441C [53]. Such modulation may be responsible for the functional loss of the domain. Other R1441x (R1441G and R1441H) mutations are not charged residues, and hence we expect similar domain modulation for those mutations [54].

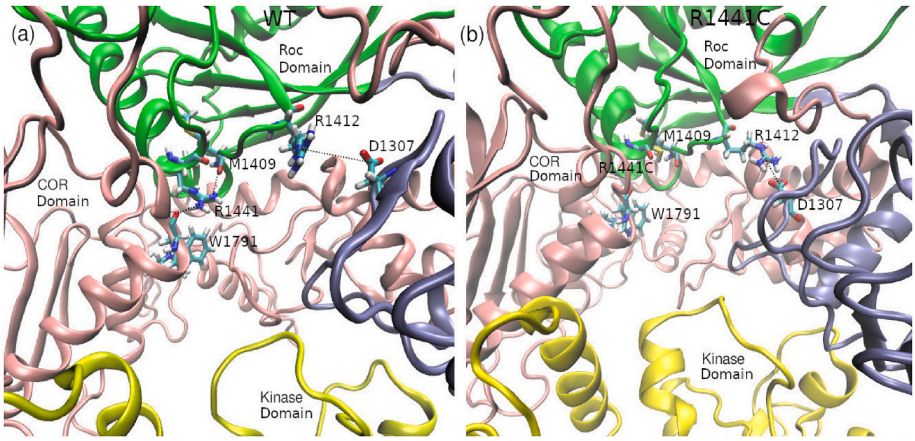

Fig. 2. Snapshots of LRRK2-WT and LRRK2[R1441C], with interacting residues represented in Licorice. (a) R1441(NH_2) - M1409(O) interaction and R1441(NH_2) – W1791(O) in the Roc and COR domains respectively. (b) Loss of R1441(NH_2) - M1409(O) and R1441(NH_2) – W1791(O) in the Roc and COR domains respectively.

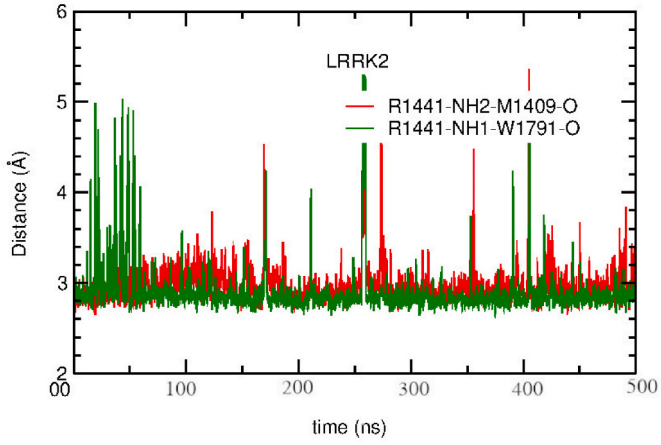

Fig. 3. The interacting distances between the sidechain nitrogen of R1441 and the carbonyl oxygen of M1409 (red) and the carbonyl oxygen of W1791(green) in LRRK2-WT.

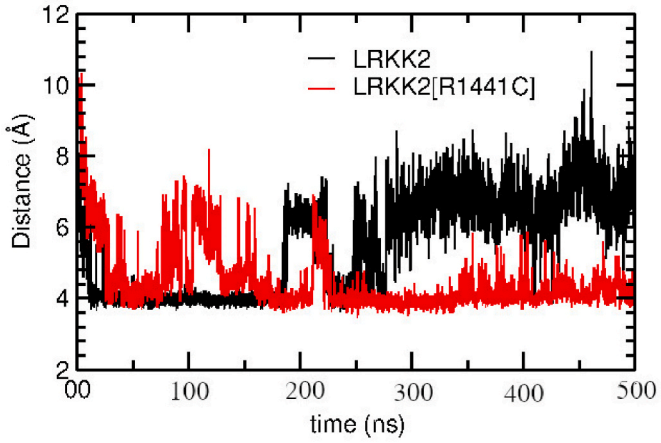

Fig. 4. R1412 (C_z) - D1307 (C_g) distances plotted for LRRK2-WT (black curve) and LRRK2[R1441C] (red curve).

3.2. Electrostatic interactions compared in LRRK2-WT and LRRK2 [D1994A] proteins

Within the Kinase domain of LRRK2-WT, we noticed an interesting observation regarding the interactions between the side chain nitrogen of the D1994 residue and the carbonyl oxygen of the T2035 residue (Fig. 6(a)).

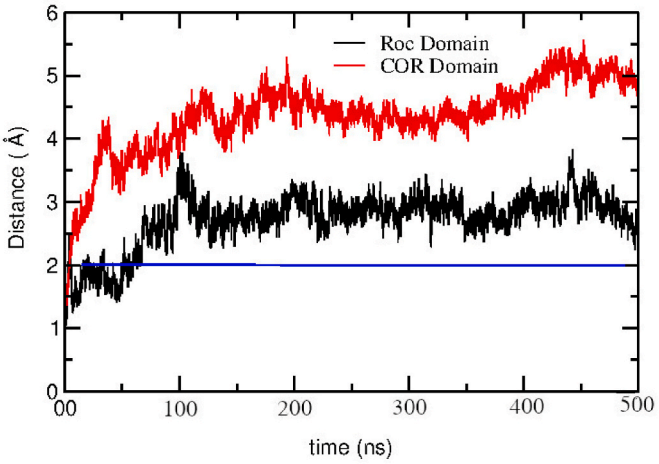

Fig. 5. RMSD of Roc domain (red) and RMSD of COR domain (black) in LRRK2 [R1441C] with respect to the average RMSD of LRRK2-WT (blue baseline).

Since the D1994 residue underwent a mutation to D1994A, carbon-carbon distances were considered. We plotted the curve for distances between the D1994(C_a)-T2035(C_a) atoms in LRRK2, and found the separation to be around 6 Å (black curve in Fig. 7). Within the kinase domain of LRRK2[D1994A], the D1994(C_a)-T2035(C_a) distance separated to 9.5 Å (red curve in Fig. 7).

Functional loss caused by the D1994A mutation may occur due to allosteric changes [53], and to attempt to understand underlying mechanisms, we investigated the changes in and around the kinase domain. We identified two residues, K1316, and R1320 in the αβ motif (Ice-Blue region in Fig. 6(a)) which form interactions with the kinase domain in the LRRK2 WT and DA mutant respectively.

K1316 forms a salt bridge with E2033 residue in the Kinase domain (black curve in Fig. 8). We observed that this interaction was lost in the presence of the D1994A mutation.

While the D1994A mutated residue resulted in loss of the E2033(C_D) - K1316(N_Z) salt bridge; it also prompted the formation of another salt bridge in Kinase domain between E2033 residue and R1320 residue (Fig. 9), which is also located in the alpha-beta motif (Ice Blue region in Fig. 6).

To observe the overall changes in the Kinase domain, the RMSD of LRRK2[D1994A] was plotted with respect to LRRK2-WT, and an average

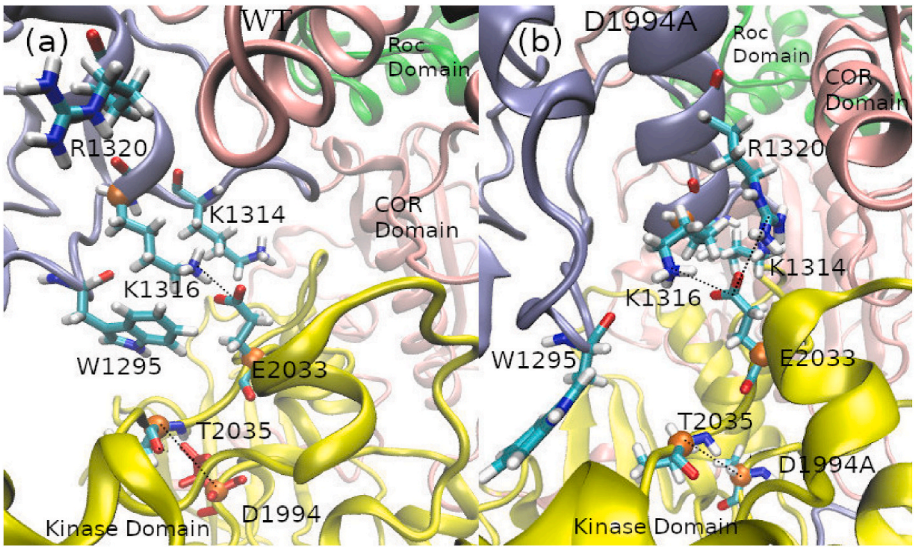

Fig. 6. Snapshots of LRRK2-WT and LRRK2[D1994A], with interacting residues represented in Licorice. (a) D1994(C_a) - T2035(C_a) interaction in the Kinase domain of LRRK2-WT. (b) D1994A(C_a) - T2035(C_a) interaction in the kinase domain of LRRK2[D1994A]. Carbon atoms of interacting residues are represented in orange in VDW representation.

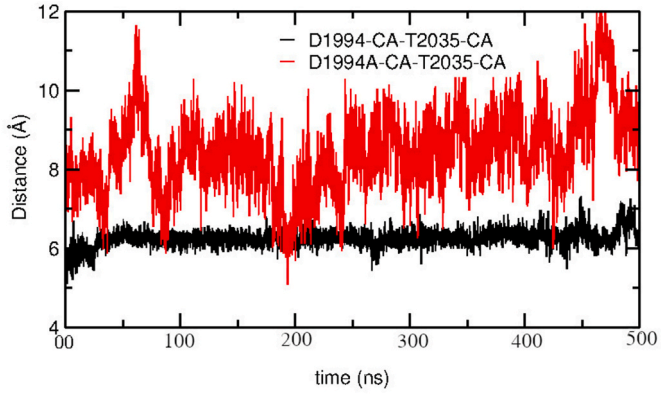

Fig. 7. D1994(C_a)-T2035(C_a) distances plotted. Distances for LRRK2-WT are shown in black, while distances for LRKK2[D1994A] are shown in red.

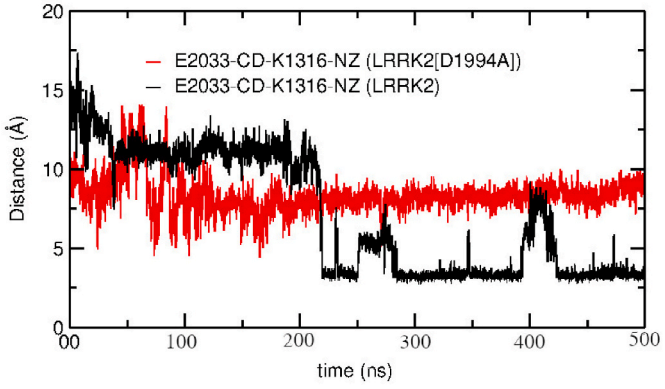

Fig. 8. E2033(C_D) - K1316(N_Z) distances. Black curve represents distances for LRRK2-WT, and the red curve represents distances for LRRK2[D1994A].

of 2.2 Å shift in RMSD was found (Fig. 10).

The artificial mutation D1994A is said to be a kinase-dead mutant [55]. The kinase domain in the inactive state is found to be unstable, aligning with our results regarding its stability [53].

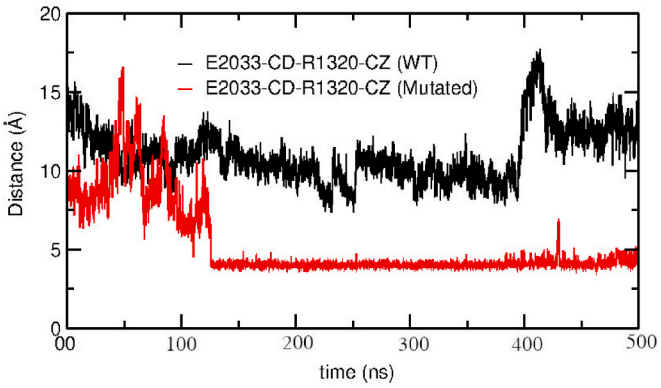

Fig. 9. The R1320 residue poorly interacts with E2033 in LRRK2-WT (black curve). The R1320 residue has strong charge interaction with E2033 in LRRK2 [D1994A] (red curve).

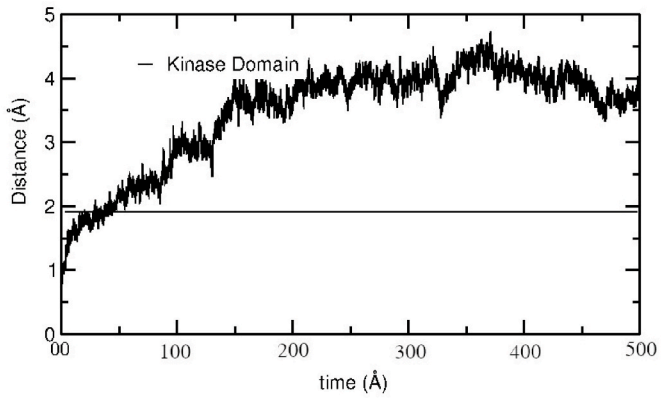

Fig. 10. RMSD of Kinase domain of LRRK2[D1994A] (black curve) compared with average RMSD of the Kinase Domain of LRRK2-WT (black horizontal line).

3.3. Electrostatic interactions compared in LRRK2-WT and LRRK2 [R1441C/D1994A] proteins

The R1441C mutation in the Roc domain is located away from the GTPase enzymatic domain, suggesting that the mutant protein's lowered GTPase activity is induced by an indirect mechanism [35]. Some studies suggest an increased kinase activity as a result [56], while others cite no significant difference between R1441C mutant and LRRK2-WT [35,57]. Regardless, an interrelation between the two catalytic domains have been well established, despite the large number of residues residing between them [22]. This begs the question – how do the effects of one domain exert a domino effect on another enzymatic domain's activity? Allosteric interactions have been identified as the mediator of this communication, according to a previous report [53]. Additionally, our results indicate the significance of the αβ motif between the LRR and Roc domains (ice-blue region in Fig. 1) in pathophysiological mechanisms. However, one question that confounds us is that the lowered GTPase activity expected for the R1441C mutant, and inactivated kinase activity for the D1994A mutant both show a strong propensity to move towards the αβ motif. To evaluate these results further, we performed a simulation introducing both mutations in a single system.

In the LRRK2-WT model, two strong and stable interactions were seen to occur between the side chain nitrogen atom of residue R1441 with the carbonyl oxygen of both M1409 and W1791, located in the Roc and COR domains respectively (Fig. 3). In line with the R1441C mutant model, both these interactions are completely lost in the double mutant system. Additionally, a strong interaction between R1412 and D1307 was observed, mimicking the same interaction in the R1441C mutant protein (Fig. 4).

Upon analysis of the kinase domain, it was found that the interaction between the side chain nitrogen of D1994 and the carbonyl oxygen of T2035 was conserved, as in the LRRK2-WT protein system(Fig. 7). Interactions observed in LRRK2-WT between E2033 and K1316 in the αβ motif (Fig. 8) was also preserved in the double mutant system. However, other interactions resulting from D1994A mutation (Fig. 9) were not conserved in the double mutant.

As shown in Figs. 11 and 12, it seems that the double mutant model preserved the interactions seen in R1441C model but lost the interactions observed in the D1994A model. These findings seem to be consistent with lowered GTPase activity and an activated kinase, despite presence of the kinase dead mutant D1994A.

To understand the stability of the domains, an RMSD of the Roc, COR, and kinase domains were plotted (Fig. 13).

The RMSD of both the Roc and COR domains showed a significant shift compared to the LRRK2 system, supporting the separation observed during GTPase underactivity [53]. Interestingly, the kinase domain displayed an average RMSD of 0.5 Å, showing increased stability as opposed to that observed in the LRRK2[D1994A] mutant. In fact, the kinase domain sustains interactions as seen in the LRRK2-WT system, suggesting that despite introduction of a kinase dead mutation, inactivation did not occur. This seems to be aligned with the results of a recent study indicating the presence of an ordered kinase domain in its active state [53] in which case, it may be postulated that an inactive kinase mutant is insufficient to override the effects of LRRK2[R1441C].

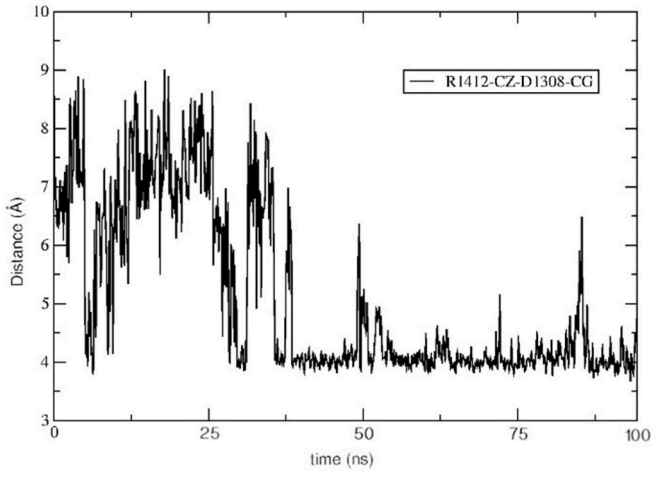

Fig. 11. Interactions between R1412(C_z)-D1307(C_g) in LRRK2 [R1441C/D1994A].

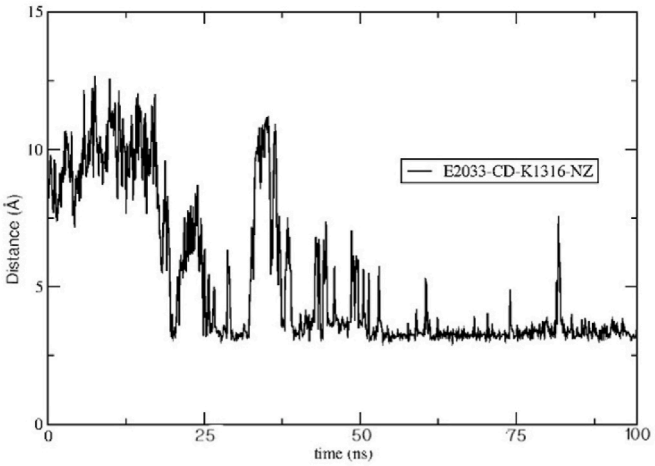

Fig. 12. Interactions between E2033(C_D)-K1316(N_Z) in LRRK2 [R1441C/D1994A].

3.3.1. Free Energy Landscapes of the αβ motifs of each system compared

All our models have the same range of 0–24 kJ/mol Gibbs free energy. The LRRK2-WT model (Fig. 14(a)) and LRRK2[R1441C/D1994A] double mutant system (Fig. 17(a)) both have one single stable conformation each. The LRRK2[R1441C] model (Fig. 15(a)) has one fully stable conformation and another partially stable conformation, while the LRRK2[D1994A] model (Fig. 16(a)) has one primary and two smaller regions with a stable conformation. On the other hand, the WT and RC models present limited variations in RMSD throughout the region, while the DA model displays a significantly higher fluctuation. Furthermore, the RMSD of the αβ motif for the RC/DA double mutant system exhibits a significantly lower RMSD (range of 0.2–1 Å) compared to its counterparts, suggesting a noteworthy increase in stability.

Given how all the models have one primary stable conformation, we speculate that none of these mutations significantly disrupts the stability of the αβ motif. In the LRRK2[R1441C] model, a primary stable conformation is observed, which may arise due to the strong R1412 (NH_2)-D1307(O) interaction obtained between the Roc domain and αβ motif (Fig. 15(b)). The LRRK2[R1441C/D1994A] double mutant system also exhibits a single stable conformation, suggesting its stability in presence of interactions of the αβ motif with both Roc and kinase domains.

On the other hand, the relatively higher RMSD of the DA mutant suggests that the αβ motif is more unstable and potentially more flexible. Additionally, the presence of several partially stable conformations indicates conformational changes corresponding to contrasting interactions formed and lost between the kinase domain and αβ motif. For instance, the interaction between residue E2033 in the kinase domain with K1316 is weaker in the mutant than in WT (Figs. 8 and 14(b)), while E2033 residue's interaction with K1314 remains similar in both systems, and E2033-E1230 interaction is gained with the introduction of D1994A mutation (Figs. 9 and 16(b)). Perhaps due to the alteration of several modifications in this region, multiple stable conformations are obtained.

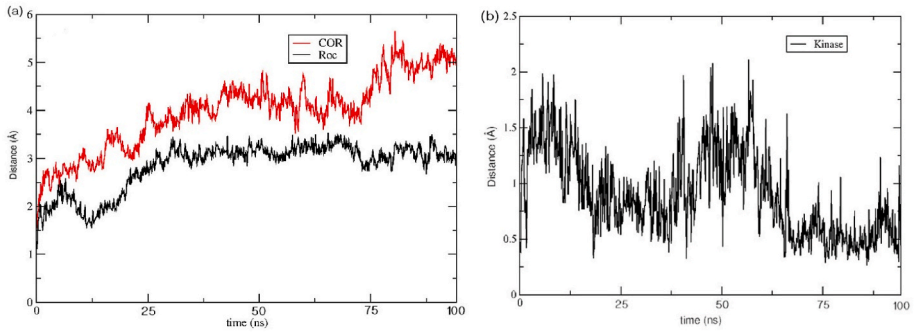

Fig. 13. (a) RMSD of Roc domain (black curve) and COR domain (red curve) in LRRK2[R1441C/D1994A]. (b) RMSD of the kinase domain in LRRK2 [R1441C/D1994A].

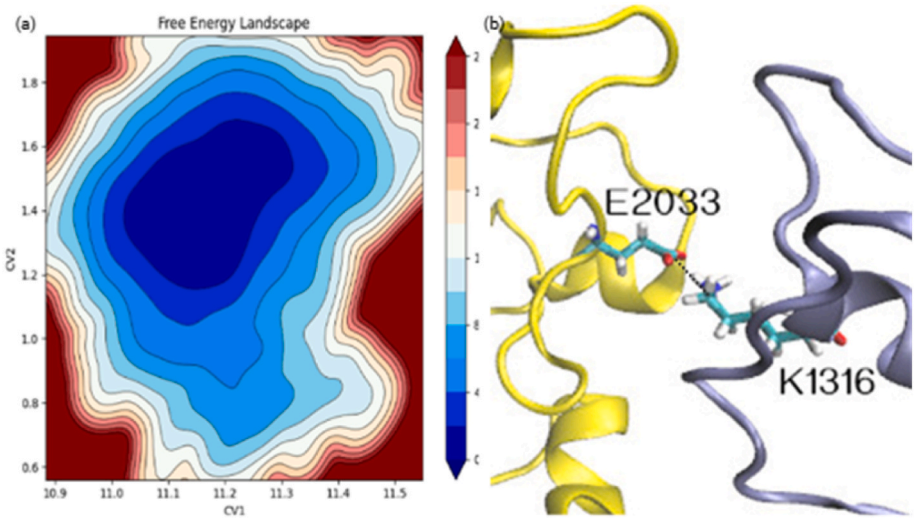

Fig. 14. (a) Free Energy Landscape (2D) for LRRK2-WT. (b) Interacting residues between kinase domain (yellow) and αβ motif (ice blue) in LRRK2-WT.

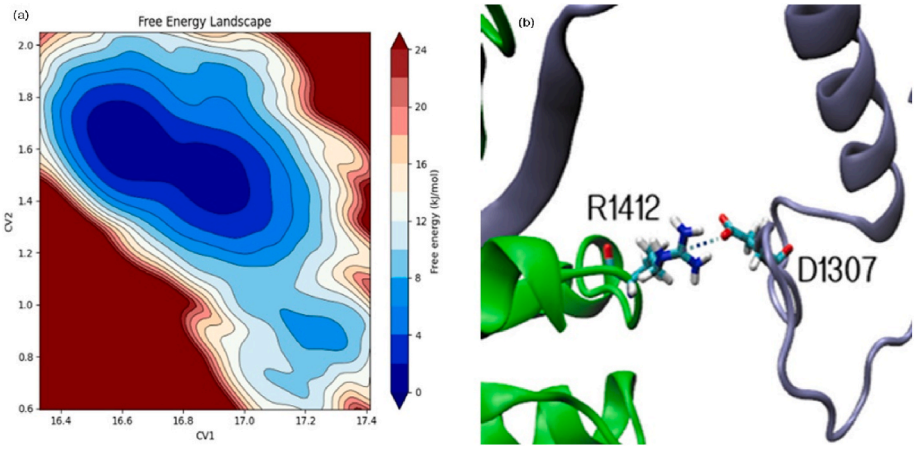

Fig. 15. (a) Free Energy Landscape (2D) for LRRK2[R1441C]. (b) Interacting residues between Roc domain (green) and αβ motif (ice blue) in LRRK2[R1441C].

4. Discussion

As a complex and large protein consisting of various motifs, LRRK2 is a dynamic system implicated in the pathogenesis of PD. Its GTPase and kinase activity is interlinked, with multiple reports of their communications [53]. In order to augment our knowledge of this complicated crosstalk, our studies involved introducing a mutation affecting the GTPase activity, R144C, and a kinase dead mutation, D1994A. Our results highlight the importance of a seemingly unlikely mediator of communication between the two domains, a strong and well-folded motif consisting an α helix and β pleated sheet adjoining the LRR and Roc domains. Both mutations studied result in loss of function of the LRRK2 protein, with the R1441C mutation dampening GTPase activity, and D1994A mutant inactivating the kinase activity.

In the R1441C mutant, observed differences with LRRK2 include a loss of interactions in the Roc domain and gain of charged interactions

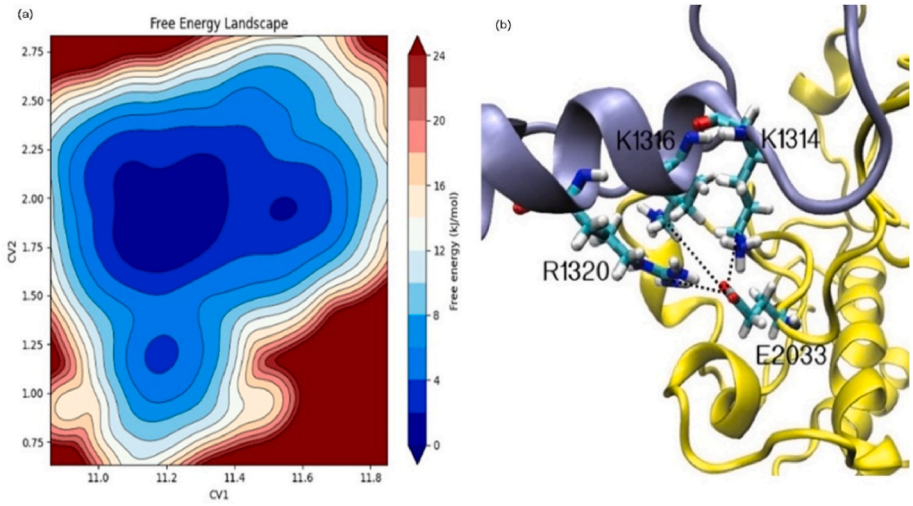

Fig. 16. (a) Free Energy Landscape (2D) for LRRK2[D1994A]. (b) Interacting residues between kinase domain (yellow) and αβ motif (ice-blue) in LRRK2[D1994A].

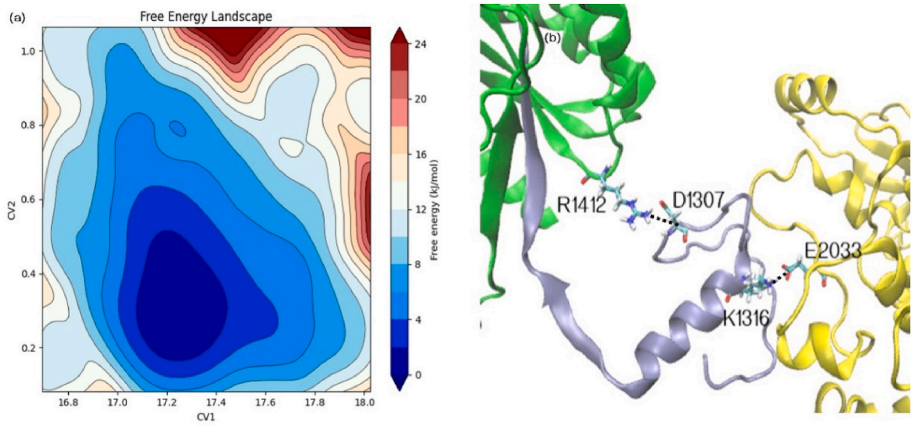

Fig. 17. (a) Free Energy Landscape (2D) of LRRK2[R1441C/D1994A]. (b) Interacting residues of R1412-D1307 between Roc domain (green) and αβ motif (ice-blue), and E2033-K1316 between kinase domain (yellow) and αβ motif (ice-blue).

with residues in the αβ motif. Similarly, the D1994A mutant also displayed a shift towards the αβ motif through gained interactions. When simulated together, the LRRK2[R1441C/D1994A] double mutant system mirrored the effects observed in the LRRK2[R1441C] mutant, and no considerable effects of LRRK2[D1994A] were identified. This may indicate that while changes in GTPase activity may affect kinase activity, the reverse effects of kinase activity on GTPase activity are insignificant [57]. In fact, since introduction of kinase dead mutation played no significant role in diminishing the effects of the R1441C mutation and failed to inactivate the domain, it is hypothesized that the therapeutic use of kinase inhibitors may not be effective for the amelioration of pathogenic mutations' effects exerted in the GTPase domain (R1441C, R1441G, R1441H, Y1699C). Furthermore, from the Free Energy Landscape analysis of the systems, it is concluded that the αβ motif is a stable part of the protein in all systems, verifying its importance.

5. Conclusion

The R1441C and D1994A mutations are both loss-of-function mutations implicated in the underactivity of the GTPase and kinase domain respectively. Interestingly, interactions with the αβ motif occur with introduction of either mutation, suggesting its role in conserving physiological functions of LRRK2. Therefore, based on our results and previous studies [55,57] focusing on the communication between these two catalytic domains, we propose that the αβ motif also plays an intermediary role. In fact, a novel mutation in this LRR-Roc linker has been identified recently [58,59], suggesting a hotspot of disease mechanisms in a part of the protein which does not directly bind the GTPase and kinase domains. Also, we emphasize the need to explore therapeutic avenues targeting GTPase impairment in LRRK2 associated PD, since interventions affecting kinase domain exerts no changes of significance in GTPase underactivity as seen in our double mutant system.

CRediT authorship contribution statement

Ramisha A. Rahman: Writing – review & editing, Writing – original draft, Investigation, Formal analysis. **Bushra Zaman:** Writing – review & editing. **Md Shariful Islam:** Writing – review & editing. **Md Harunur Rashid:** Writing – review & editing, Writing – original draft, Supervision, Project administration, Investigation, Formal analysis, Conceptualization.

Declaration of competing interest

The authors declare that they have no known competing financial interests or personal relationships that could have appeared to influence the work reported in this paper.

Acknowledgements

The authors express gratitude to the in-house computing facilities provided by NSU as well the NSU CTRG grant ID: CTRG-23-SEPS-14. We also acknowledge the UNESCO TWAS 2024 Individual Research Grant. Biorender.com was used to create Fig. 1(a) graphic. In addition, we acknowledge Mohammad Radid Khan, Research Assistant at North South University for his contribution to the FEL analysis.

References

[1] C. Váradi, Clinical features of Parkinson's disease: the evolution of critical symptoms, Biology 9 (2020), https://doi.org/10.3390/biology9050103.
[2] A.H.V. Schapira, K.R. Chaudhuri, P. Jenner, Non-motor features of Parkinson disease, Nat. Rev. Neurosci. 18 (2017) 435–450, https://doi.org/10.1038/nrn.2017.62.
[3] Antonia Kouli, Kelli M. Torsney, Wei-Li kuan, Parkinson's disease: etiology, neuropathology, and pathogenesis, in: Parkinson's Disease: Pathogenesis and Clinical Aspects, Codon Publications, 2018.
[4] X. Dong-Chen, C. Yong, X. Yang, S.T. Chen-Yu, P. Li-Hua, Signaling pathways in Parkinson's disease: molecular mechanisms and therapeutic interventions, Signal Transduct. Targeted Ther. 8 (2023), https://doi.org/10.1038/s41392-023-01353-3.
[5] C.H. Langley, B. Charlesworth, Nature © Macmillan Publishers Ltd 1997 Expansion of Xenotransplantation, 1997.
[6] L. Stefanis, α-Synuclein in Parkinson's disease, Cold Spring Harb Perspect Med 2 (2012), https://doi.org/10.1101/cshperspect.a009399.
[7] Genetics & Parkinson's, Parkinson's foundation, Available at: https://www.parkinson.org/understanding-parkinsons/causes/genetics. (Accessed 26 October 2024).
[8] C. Blauwendraat, M.A. Nalls, A.B. Singleton, The genetic architecture of Parkinson's disease, Lancet Neurol. 19 (2020) 170–178, https://doi.org/10.1016/S1474-4422(19)30287-X.
[9] M. Funayama, K. Nishioka, Y. Li, N. Hattori, Molecular genetics of Parkinson's disease: Contributions and global trends, J. Hum. Genet. 68 (2023) 125–130, https://doi.org/10.1038/s10038-022-01058-5.
[10] E.K. Tan, L.M. Skipper, Pathogenic mutations in Parkinson disease, Hum. Mutat. 28 (2007) 641–653, https://doi.org/10.1002/humu.20507.
[11] C.M. Lill, Genetics of Parkinson's disease, Mol. Cell. Probes 30 (2016) 386–396, https://doi.org/10.1016/j.mcp.2016.11.001.
[12] C. Paisán-Ruiz, A. Li, S.A. Schneider, J.L. Holton, R. Johnson, D. Kidd, J. Chataway, K.P. Bhatia, A.J. Lees, J. Hardy, T. Revesz, H. Houlden, Widespread Lewy body and tau accumulation in childhood and adult onset dystonia-parkinsonism cases with PLA2G6 mutations, Neurobiol. Aging 33 (2012) 814–823, https://doi.org/10.1016/j.neurobiolaging.2010.05.009.
[13] A. Zimprich, S. Biskup, P. Leitner, P. Lichtner, M. Farrer, S. Lincoln, J. Kachergus, M. Hulihan, R.J. Uitti, D.B. Calne, A.J. Stoessl, Mutations in LRRK2 cause autosomal-dominant parkinsonism with pleomorphic pathology families, Neuron 44 (2004) 601–607. http://www.neuron.org/cgi/content/full/44/4/.
[14] C. Paisá N-Ruíz, S. Jain, E.W. Evans, W.P. Gilks, J. Simó, M. Van Der Brug, A. Ló Pez De Munain, S. Aparicio, A.M. Gil, N. Khan, J. Johnson, J. Ruiz Martinez, D. Nicholl, Cloning of the gene containing mutations that cause PARK8-linked Parkinson's disease, Neuron 44 (2004) 595–600.
[15] A. Usmani, F. Shavarebi, A. Hiniker, The cell biology of LRRK2 in Parkinson's disease, Mol. Cell Biol. 41 (2021), https://doi.org/10.1128/mcb.00660-20.
[16] J. Jankovic, E.K. Tan, Parkinson's disease: etiopathogenesis and treatment, J. Neurol. Neurosurg. Psychiatry 91 (2020) 795–808, https://doi.org/10.1136/jnnp-2019-322338.
[17] X. Zhu, A. Babar, S.L. Siedlak, Q. Yang, G. Ito, T. Iwatsubo, M.A. Smith, G. Perry, S. G. Chen, LRRK2 in Parkinson's disease and dementia with Lewy bodies, Mol. Neurodegener. 1 (2006), https://doi.org/10.1186/1750-1326-1-17.
[18] P. Zhang, Y. Fan, H. Ru, L. Wang, V.G. Magupalli, S.S. Taylor, D.R. Alessi, H. Wu, Crystal structure of the WD40 domain dimer of LRRK2, Proc. Natl. Acad. Sci. U. S. A. 116 (2019) 1579–1584, https://doi.org/10.1073/pnas.1817889116.
[19] K. Harvey, T.F. Outeiro, The role of LRRK2 in cell signalling, Biochem. Soc. Trans. 47 (2018) 197–207, https://doi.org/10.1042/BST20180464.
[20] M.R. Cookson, The role of leucine-rich repeat kinase 2 (LRRK2) in Parkinson's disease, Nat. Rev. Neurosci. 11 (2010) 791–797, https://doi.org/10.1038/nrn2935.
[21] I.F. Mata, W.J. Wedemeyer, M.J. Farrer, J.P. Taylor, K.A. Gallo, LRRK2 in Parkinson's disease: protein domains and functional insights, Trends Neurosci. 29 (2006) 286–293, https://doi.org/10.1016/j.tins.2006.03.006.
[22] Y. Xiong, V.L. Dawson, T.M. Dawson, LRRK2 GTPase dysfunction in the pathogenesis of Parkinson's disease, Biochem. Soc. Trans. 40 (2012) 1074–1079, https://doi.org/10.1042/BST20120093.
[23] D.G. Healy, M. Falchi, S.S. O'sullivan, V. Bonifati, A. Durr, S. Bressman, A. Brice, J. Aasly, C.P. Zabetian, S. Goldwurm, J.J. Ferreira, E. Tolosa, D.M. Kay, C. Klein, D. R. Williams, C. Marras, A.E. Lang, Z.K. Wszolek, J. Berciano, A.H. Schapira, T. Lynch, K.P. Bhatia, T. Gasser, A.J. Lees, N.W. Wood, Articles Phenotype, genotype, and worldwide genetic penetrance of LRRK2-associated Parkinson's disease: a case-control study, 583, https://doi.org/10.1016/S1474, 2008.
[24] A.J. Lees, J. Hardy, T. Revesz, Parkinson's disease, Lancet 373 (2009) 2055–2066, https://doi.org/10.1016/S0140-6736(09)60492-X.
[25] M.S. Islam, D.J. Moore, Mechanisms of LRRK2-dependent neurodegeneration: role of enzymatic activity and protein aggregation, Biochem. Soc. Trans. 45 (2017) 163–172, https://doi.org/10.1042/BST20160264.
[26] D.C. Berwick, K. Harvey, LRRK2 signaling pathways: the key to unlocking neurodegeneration? Trends Cell Biol. 21 (2011) 257–265, https://doi.org/10.1016/j.tcb.2011.01.001.
[27] Y. Xiong, C.E. Coombes, A. Kilaru, X. Li, A.D. Gitler, W.J. Bowers, V.L. Dawson, T. M. Dawson, D.J. Moore, GTPase activity plays a key role in the pathobiology of LRRK2, PLoS Genet. 6 (2010), https://doi.org/10.1371/journal.pgen.1000902.
[28] I. Martin, J.W. Kim, V.L. Dawson, T.M. Dawson, LRRK2 pathobiology in Parkinson's disease, J. Neurochem. 131 (2014) 554–565, https://doi.org/10.1111/jnc.12949.
[29] D.C. Berwick, K. Harvey, LRRK2 signaling pathways: the key to unlocking neurodegeneration? Trends Cell Biol. 21 (2011) 257–265, https://doi.org/10.1016/j.tcb.2011.01.001.
[30] E.V. Nikonova, Y. Xiong, K.Q. Tanis, V.L. Dawson, R.L. Vogel, E.M. Finney, D. J. Stone, I.J. Reynolds, J.T. Kern, T.M. Dawson, Transcriptional responses to loss or gain of function of the leucine-rich repeat kinase 2 (LRRK2) gene uncover biological processes modulated by LRRK2 activity, Hum. Mol. Genet. 21 (2012) 163–174, https://doi.org/10.1093/hmg/ddr451.
[31] Z.K. Wszolek, B. Pfeiffer, J.R. Fulgham, J.E. Parisi, B.M. Thompson, R.J. Uitti, D. B. Calne, R.F. Pfeiffer, Western Nebraska family (family D) with autosomal dominant parkinsonism, Neurology 45 (1995) 502–505.
[32] K. Haugarvoll, R. Rademakers, J.M. Kachergus, K. Nuytemans, O.A. Ross, J. M. Gibson, E.K. Tan, C. Gaig, E. Tolosa, S. Goldwurm, M. Guidi, G. Riboldazzi, L. Brown, U. Walter, R. Benecke, D. Berg, T. Gasser, J. Theuns, P. Pals, P. Cras, P. P. De Deyn, S. Engelborghs, B. Pickut, R.J. Uitti, T. Foroud, W.C. Nichols, J. Hagenah, C. Klein, A. Samii, C.P. Zabetian, V. Bonifati, C. Van Broeckhoven, M. J. Farrer, Z.K. Wszolek, Lrrk2 R1441C parkinsonism is clinically similar to sporadic Parkinson disease, Neurology 70 (2008) 1456–1460, https://doi.org/10.1212/01.wnl.0000304044.22253.03.
[33] M.S. Islam, H. Nolte, W. Jacob, A.B. Ziegler, S. Pütz, Y. Grosjean, K. Szczepanowska, A. Trifunovic, T. Braun, H. Heumann, R. Heumann, B. Hovemann, D.J. Moore, M. Krüger, Human R1441C LRRK2 regulates the synaptic vesicle proteome and phosphoproteome in a Drosophila model of Parkinson's disease, Hum. Mol. Genet. 25 (2016) 5365–5382, https://doi.org/10.1093/hmg/ddw352.
[34] Y. Tong, A. Pisani, G. Martella, M. Karouani, H. Yamaguchi, E.N. Pothos, J. Shen, R1441C mutation in LRRK2 impairs dopaminergic neurotransmission in mice, Proc. Natl. Acad. Sci. U. S. A. 106 (2009) 14622–14627. www.pnas.orgcgidoi10.1073pnas.0906334106.
[35] P.A. Lewis, E. Greggio, A. Beilina, S. Jain, A. Baker, M.R. Cookson, The R1441C mutation of LRRK2 disrupts GTP hydrolysis, Biochem. Biophys. Res. Commun. 357 (2007) 668–671, https://doi.org/10.1016/j.bbrc.2007.04.006.
[36] F. Cardona, M. Tormos-Pérez, J. Pérez-Tur, Structural and functional in silico analysis of LRRK2 missense substitutions, Mol. Biol. Rep. 41 (2014) 2529–2542, https://doi.org/10.1007/s11033-014-3111-z.
[37] X. Li, Z. Qi, D. Ni, S. Lu, L. Chen, X. Chen, Markov state models and molecular dynamics simulations provide understanding of the nucleotide-dependent dimerization-based activation of lrrk2 roc domain, Molecules 26 (2021), https://doi.org/10.3390/molecules26185647.
[38] Y.L. Sosero, Z. Gan-Or, LRRK2 and Parkinson's disease: from genetics to targeted therapy, Ann Clin Transl Neurol 10 (2023) 850–864, https://doi.org/10.1002/acn3.51776.
[39] R. Watanabe, R. Buschauer, J. Böhning, M. Audagnotto, K. Lasker, T.W. Lu, D. Boassa, S. Taylor, E. Villa, The in situ structure of Parkinson's disease-linked LRRK2, Cell 182 (2020) 1508–1518.e16, https://doi.org/10.1016/j.cell.2020.08.004.
[40] E. Ray Dorsey, A. Elbaz, E. Nichols, F. Abd-Allah, A. Abdelalim, J.C. Adsuar, M. G. Ansha, C. Brayne, J.Y.J. Choi, D. Collado-Mateo, N. Dahodwala, H.P. Do, D. Edessa, M. Endres, S.M. Fereshtehnejad, K.J. Foreman, F.G. Gankpe, R. Gupta, G.J. Hankey, S.I. Hay, M.I. Hegazy, D.T. Hibstu, A. Kasaeian, Y. Khader, I. Khalil, Y. H. Khang, Y.J. Kim, Y. Kokubo, G. Logroscino, J. Massano, N.M. Ibrahim, M. A. Mohammed, A. Mohammadi, M. Moradi-Lakeh, M. Naghavi, B.T. Nguyen, Y. L. Nirayo, F.A. Ogbo, M.O. Owolabi, D.M. Pereira, M.J. Postma, M. Qorbani, M. A. Rahman, K.T. Roba, H. Safari, S. Safiri, M. Satpathy, M. Sawhney, A. Shafieesabet, M.S. Shiferaw, M. Smith, C.E.I. Szoeke, R. Tabarés-Seisdedos, N. T. Truong, K.N. Ukwaja, N. Venketasubramanian, S. Villafaina, K.G. Weldegwergs, R. Westerman, T. Wijeratne, A.S. Winkler, B.T. Xuan, N. Yonemoto, V.L. Feigin, T. Vos, C.J.L. Murray, Global, regional, and national burden of Parkinson's disease, 1990–2016: a systematic analysis for the Global Burden of Disease Study 2016, Lancet Neurol. 17 (2018) 939–953, https://doi.org/10.1016/S1474-4422(18)30295-3.
[41] S.J. Chia, E.K. Tan, Y.X. Chao, Historical perspective: models of Parkinson's disease, Int. J. Mol. Sci. 21 (2020), https://doi.org/10.3390/ijms21072464.
[42] R.A. Rahman, B. Zaman, M.R. Khan, M.S. Islam, M.H. Rashid, Computational studies show how the H463R mutation turns hKv1.5 into an inactivation state, J. Phys. Chem. B 128 (2024) 429–439, https://doi.org/10.1021/acs.jpcb.3c05634.
[43] M.H. Rashid, R. Huq, M.R. Tanner, S. Chhabra, K.K. Khoo, R. Estrada, V. Dhawan, S. Chauhan, M.W. Pennington, C. Beeton, S. Kuyucak, R.S. Norton, A potent and Kv1.3-selective analogue of the scorpion toxin HsTX1 as a potential therapeutic for autoimmune diseases, Sci. Rep. 4 (2014), https://doi.org/10.1038/srep04509.
[44] M.H. Rashid, S. Mahdavi, S. Kuyucak, Computational studies of marine toxins targeting ion channels, Mar. Drugs 11 (2013) 848–869, https://doi.org/10.3390/md11030848.

[45] M.H. Rashid, S. Kuyucak, Computational study of the loss-of-function mutations in the Kv1.5 channel associated with atrial fibrillation, ACS Omega 3 (2018) 8882–8890, https://doi.org/10.1021/acsomega.8b01094.
[46] M.H. Rashid, Molecular simulation of the Kv7.4[ΔS269] mutant channel reveals that ion conduction in the cavity is perturbed due to hydrophobic gating, Biochem Biophys Rep 25 (2021), https://doi.org/10.1016/j.bbrep.2020.100879.
[47] M. Karplus, G. Petsko, Molecular dynamics simulations in biology, Nature 347 (1990) 631–639, https://doi.org/10.1038/347631a0.
[48] A. Myasnikov, H. Zhu, P. Hixson, B. Xie, K. Yu, A. Pitre, J. Peng, J. Sun, Structural analysis of the full-length human LRRK2, Cell 184 (2021) 3519–3527.e10, https://doi.org/10.1016/j.cell.2021.05.004.
[49] J.C. Phillips, D.J. Hardy, J.D.C. Maia, J.E. Stone, J.V. Ribeiro, R.C. Bernardi, R. Buch, G. Fiorin, J. Hénin, W. Jiang, R. McGreevy, M.C.R. Melo, B.K. Radak, R. D. Skeel, A. Singharoy, Y. Wang, B. Roux, A. Aksimentiev, Z. Luthey-Schulten, L. V. Kalé, K. Schulten, C. Chipot, E. Tajkhorshid, Scalable molecular dynamics on CPU and GPU architectures with NAMD, J. Chem. Phys. 153 (2020), https://doi.org/10.1063/5.0014475.
[50] B.R. Brooks, C.L. Brooks, A.D. Mackerell, L. Nilsson, R.J. Petrella, B. Roux, Y. Won, G. Archontis, C. Bartels, S. Boresch, A. Caflisch, L. Caves, Q. Cui, A.R. Dinner, M. Feig, S. Fischer, J. Gao, M. Hodoscek, W. Im, K. Kuczera, T. Lazaridis, J. Ma, V. Ovchinnikov, E. Paci, R.W. Pastor, C.B. Post, J.Z. Pu, M. Schaefer, B. Tidor, R. M. Venable, H.L. Woodcock, X. Wu, W. Yang, D.M. York, M. Karplus, CHARMM: the biomolecular simulation program, J. Comput. Chem. 30 (2009) 1545–1614, https://doi.org/10.1002/jcc.21287.
[51] J. Lee, X. Cheng, J.M. Swails, M.S. Yeom, P.K. Eastman, J.A. Lemkul, S. Wei, J. Buckner, J.C. Jeong, Y. Qi, S. Jo, V.S. Pande, D.A. Case, C.L. Brooks, A. D. MacKerell, J.B. Klauda, W. Im, CHARMM-GUI input generator for NAMD, GROMACS, AMBER, OpenMM, and CHARMM/OpenMM simulations using the CHARMM36 additive force field, J. Chem. Theor. Comput. 12 (2016) 405–413, https://doi.org/10.1021/acs.jctc.5b00935.
[52] W. Humphrey, A. Dalke, K. Schulten, VMD: visual molecular dynamics, J. Mol. Graph. 14 (1996) 33–38.
[53] J.H. Weng, P.C. Aoto, R. Lorenz, J. Wu, S.H. Schmidt, J.T. Manschwetus, P. Kaila-Sharma, S. Silletti, S. Mathea, D. Chatterjee, S. Knapp, F.W. Herberg, S.S. Taylor, LRRK2 dynamics analysis identifies allosteric control of the crosstalk between its catalytic domains, PLoS Biol. 20 (2022), https://doi.org/10.1371/journal.pbio.3001427.
[54] K. Muda, D. Bertinetti, F. Gesellchen, J.S. Hermann, F. Von Zweydorf, A. Geerlof, A. Jacob, M. Ueffing, C.J. Gloeckner, F.W. Herberg, Parkinson-related LRRK2 mutation R1441C/G/H impairs PKA phosphorylation of LRRK2 and disrupts its interaction with 14-3-3, Proc. Natl. Acad. Sci. U. S. A. 111 (2014) E34–E43, https://doi.org/10.1073/pnas.1312701111.
[55] A. Phu Tran Nguyen, E. Tsika, K. Kelly, N. Levine, X. Chen, A.B. West, S. Boularand, P. Barneoud, D.J. Moore, Dopaminergic neurodegeneration induced by Parkinson's disease-linked G2019S LRRK2 is dependent on kinase and GTPase activity, Proc. Natl. Acad. Sci. U. S. A. 117 (2020) 17296–17307, https://doi.org/10.1073/pnas.1922184117/-/DCSupplemental.
[56] A.B. West, D.J. Moore, S. Biskup, A. Bugayenko, W.W. Smith, C.A. Ross, V. L. Dawson, T.M. Dawson, Parkinson's disease-associated mutations in leucine-rich repeat kinase 2 augment kinase activity, Proc. Natl. Acad. Sci. U. S. A. 102 (2005) 16842–16847. www.pnas.orgcgidoi10.1073pnas.0507360102.
[57] A. Biosa, A. Trancikova, L. Civiero, L. Glauser, L. Bubacco, E. Greggio, D.J. Moore, GTPase activity regulates kinase activity and cellular phenotypes of Parkinson's disease-associated LRRK2, Hum. Mol. Genet. 22 (2013) 1140–1156, https://doi.org/10.1093/hmg/dds522.
[58] E. Stormer, J.H. Weng, J. Wu, D. Bertinetti, P.K. Sharma, W. Ma, F.W. Herberg, S. S. Taylor, Capturing the domain crosstalk in full length LRRK2 and LRRK2RCKW, Biochem. J. 480 (2023) 815–833, https://doi.org/10.1042/BCJ20230126.
[59] J.H. Weng, C.R. Trilling, P. Kaila Sharma, E. Störmer, J. Wu, F.W. Herberg, S. S. Taylor, Novel LRR-ROC motif that links the N- and C-terminal domains in LRRK2 undergoes an order–disorder transition upon activation, J. Mol. Biol. 435 (2023) 168485, https://doi.org/10.1016/j.jmb.2023.167999.